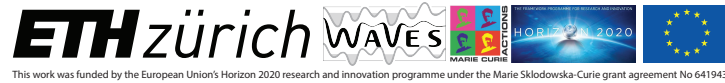


Physical Implementation of Immersive Boundary Conditions in 1D (4aSAb9)

Theodor S. Becker^{1*}, Dirk-Jan van Manen¹, Carly M. Donahue¹, Johan O.A. Robertsson¹
¹Exploration and Environmental Geophysics, Department of Earth Sciences, ETH Zurich



This work was funded by the European Union's Horizon 2020 research and innovation programme under the Marie Skłodowska-Curie grant agreement No 641943



*email: theodor.becker@erdw.ethz.ch

1 Introduction

Most wave propagation laboratories suffer from size-related limitations, e.g., due to strong reflections of the wavefield at the laboratory boundary, which imposes restrictions on the maximum wavelength of the probing signal. We currently construct a novel wave propagation laboratory that circumvents this issue by actively suppressing reflections from the laboratory boundary using the method of immersive boundary conditions (IBCs)^{1,2}. Additionally, IBCs enable immersion of the physical laboratory in a virtual domain enclosing the laboratory. Here, we present first results of the physical implementation of IBCs on one side of a one-dimensional wave guide.

2 Concept of IBCs

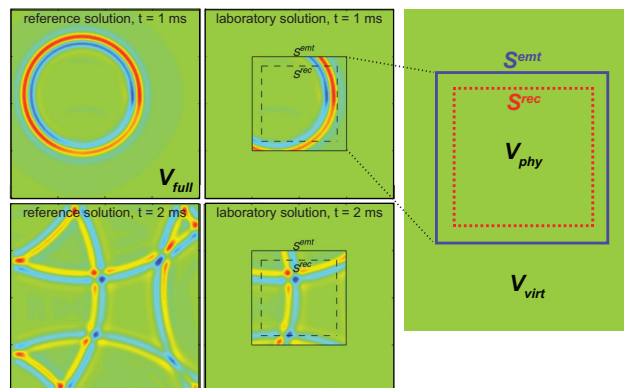


Fig. 1. We consider three different domains: the physical laboratory V_{phy} , a virtual domain V_{virt} enclosing V_{phy} , and a full domain V_{full} in which both domains are linked by a transparent boundary. Further consider an emitting surface S^{emt} coinciding with the rigid boundary of V_{phy} and a recording surface S^{rec} slightly inside V_{phy} . Figure modified after Vasmel et al. (2013).

- differencing pressure fields in V_{full} and V_{phy} and assuming a rigid laboratory boundary on S^{emt} yields:

$$p^{IBC}(\mathbf{x}', t) = \bar{p}(\mathbf{x}', t) - p(\mathbf{x}', t) = - \oint_{S^{emt}} [G^{p,q}(\mathbf{x}', \mathbf{x}, t) * \bar{v}_i(\mathbf{x}, t)] n_i dS, \text{ for } \mathbf{x}' \in V_{phy} \quad (1)$$

- i.e., IBCs are enforced by injecting monopole sources on S^{emt} weighted by the normal particle velocity of V_{full} on S^{emt}
- the normal particle velocity of V_{full} on S^{emt} can be predicted using a Kirchhoff-Helmholtz extrapolation integral:

$$\bar{v}_i(\mathbf{x}^{emt}, t) = \oint_{S^{rec}} [\bar{G}_i^{v,q}(\mathbf{x}^{emt}, \mathbf{x}, t) * \bar{v}_m(\mathbf{x}, t) + \bar{G}_i^{v,f}(\mathbf{x}^{emt}, \mathbf{x}, t) * \bar{p}(\mathbf{x}, t)] n_m dS \quad (2)$$

- the recursive, time-descretized equivalent of equation (2), pressure and particle velocity measurements on S^{rec} and monopole and dipole impulse responses of V_{full} from S^{rec} to S^{emt} are required for the IBC implementation.

3 Physical implementation

The extrapolation engine

A physical implementation of IBCs requires the evaluation of equation (2) in real-time. To meet the strict timing requirements, a high-performance data acquisition and control system driven by field-programmable gate arrays (FPGAs) is used for the IBC computation (see Fig. 2).

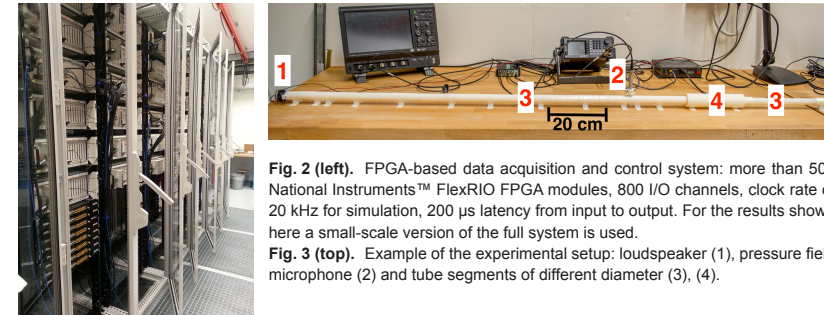


Fig. 2 (left). FPGA-based data acquisition and control system: more than 500 National Instruments™ FlexRIO FPGA modules, 800 I/O channels, clock rate of 20 kHz for simulation, 200 μ s latency from input to output. For the results shown here a small-scale version of the full system is used.

Fig. 3 (top). Example of the experimental setup: loudspeaker (1), pressure field microphone (2) and tube segments of different diameter (3), (4).

The 1D laboratory

IBCs are implemented on one side of an air-filled circular tube of variable diameter (see Fig. 3). Two loudspeakers create a one-dimensional wavefield inside the tube and inject the IBCs, respectively. We use two pressure field microphones at S^{rec} to record the pressure and derive the normal particle velocity. The pressure along the tube is measured with a third microphone.

4 Results (1)

- Ricker wavelets with 1 kHz to 5 kHz center frequency are injected into the wave guide depicted in Fig. 6 with a stimulus loudspeaker (left)
- IBCs are injected with a second loudspeaker (right)
- the extrapolation Green's functions include inverse source transfer function, particle velocity approximation, pressure interpolation, a calibration filter and the reflectivity of IBC loudspeaker

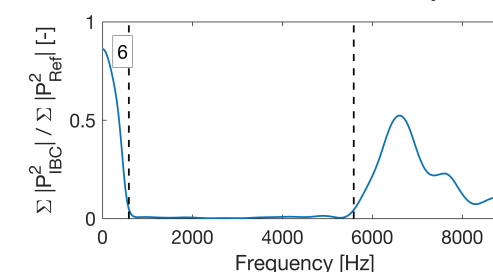


Fig. 4. Ratio of the squared absolute pressure values in a window around the reflected wave with respect to the reference case, where the IBC loudspeaker is inactive - summed over five experiments for Ricker wavelets with 1 kHz to 5 kHz center frequency.

5 Results (2)

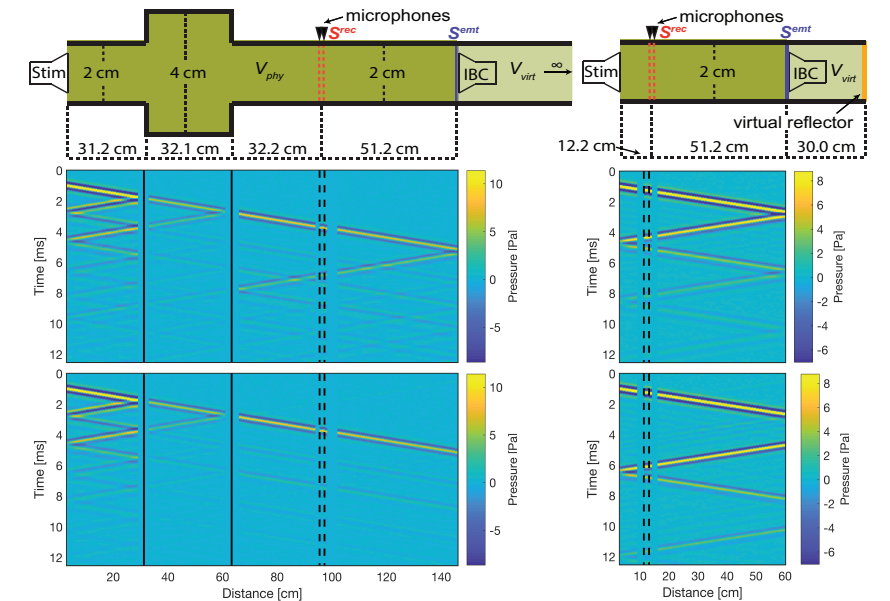


Fig. 5. Waveguide geometry (top), reference wavefield (center) and wavefield with active IBCs representing a homogeneous background medium (bottom).

Fig. 6. Waveguide geometry (top), reference wavefield (center) and wavefield with active IBCs representing a truncated background medium (bottom).

6 Discussion and conclusions

- >95% reflected energy suppressed between 0.5 kHz and 5.5 kHz
- immersive wave propagation captures interactions between physical and virtual domain (*virtual extension of the wave guide*)
- residual energy from emitting boundary due to imperfect removal of the source signature, limited spatial and temporal sampling, incomplete correction for attenuation, re-assembling of the wave guide
- two-sided 1D, as well as 2D and 3D experiments are currently underway

7 References

- ¹ van Manen, D.-J., Robertsson, J. O. A., and Curtis, A. (2007). Exact wave field simulation for finite-volume scattering problems. *Journal of Acoustic Society of America*, 122(October):EL115–L121.
- ² Vasmel, M., Robertsson, J. O. A., van Manen, D.-J., and Curtis, A. (2013). Immersive experimentation in a wave propagation laboratory. *Journal of Acoustic Society of America*, 134(6):EL492.